ISSN 1063-7826, Semiconductors, 2016, Vol. 50, No. 5, pp. 652–655. © Pleiades Publishing, Ltd., 2016.
Original Russian Text © E.V. Nikitina, A.S. Gudovskikh, A.A. Lazarenko, E.V. Pirogov, M.S. Sobolev, K.S. Zelentsov, I.A. Morozov, A.Yu. Egorov, 2016, published in Fizika i Tekhnika Poluprovodnikov, 2016, Vol. 50, No. 5, pp. 663–667.

PHYSICS OF SEMICONDUCTOR DEVICES

GaAs/InGaAsN Heterostructures for Multi-Junction Solar Cells

E. V. Nikitina[a]*, A. S. Gudovskikh[a, b], A. A. Lazarenko[a], E. V. Pirogov[a], M. S. Sobolev[a], K. S. Zelentsov[a], I. A. Morozov[a], and A. Yu. Egorov[c]

[a] *St. Petersburg National Research Academic University, Russian Academy of Sciences, St. Petersburg, 194021 Russia*
[b] *St. Petersburg State Electrotechnical University LETI, St. Petersburg, 197376 Russia*
[c] *St. Petersburg National Research University of Information Technologies, Mechanics, and Optics ITMO, St. Petersburg, 197101 Russia*
**e-mail: nikitina@mail.ru*

Submitted October 7, 2015; accepted for publication October 16, 2015

Abstract—Solar-cell heterostructures based on GaAs/InGaAsN materials with an InAs/GaAsN superlattice, grown by molecular beam epitaxy, are studied. A *p*-GaAs/*i*-(InAs/GaAsN)/*n*-GaAs *p*–*i*–*n* test solar cell with a 0.9-μm-thick InGaAsN layer has an open-circuit voltage of 0.4 V (1 sun, AM1.5G) and a quantum efficiency of >0.75 at a wavelength of 940 nm (at zero reflection loss), which corresponds to a short-circuit current of 26.58 mA/cm^2 (AM1.5G, 100 mW/cm^2). The high open-circuit voltage demonstrates that InGaAsN can be used as a material with a band gap of 1 eV in four-cascade solar cells.

DOI: 10.1134/S106378261605016X

1. INTRODUCTION

Lattice-matched three-junction GaInP/GaInAs/Ge solar cells with high crystal perfection at present make up the majority of industrially manufactured high-efficiency multi-junction solar cells. The efficiency of three-junction GaInP/GaAs/Ge solar-cell arrays exceeds 40%, which is close to the theoretical limit [1]. Theoretical estimates have shown that the efficiency of multi-junction solar cells lattice-matched with Ge substrates can be raised to 52% by adding one more junction with a band gap of ~1 eV [2]. The ternary solution $Ga_{0.93}In_{0.07}N_{0.02}As_{0.98}$ (henceforth GaInNAs) is the most attractive material lattice-matched with GaAs and has the necessary band gap [3]. However, the addition of nitrogen markedly impairs the quality of the material of GaInNAs layers [4, 5]. The problems associated with the application of this material consist in the poor transport characteristics of currently attainable InGaAsN layers (diffusion length ~10–20 nm). To improve the crystal quality and transport characteristics, antimony is added to InGaAsN layers and a solid solution composed of five elements, InGaAsNSb, is formed [6]. The world record for efficiency was achieved using lattice-matched three-junction GaInP/GaAs/InGaAsNSb solar cells [7]. However, antimony has a clearly pronounced "memory effect" and accumulates on growth reactor walls, which leads to its incorporation into the layers of subsequent cascades. Being an isovalent impurity, antimony creates additional recombination centers, which impairs the photoelectric characteristics of the upper cascades. To preclude the adverse effect of antimony, the upper cascades should be grown in a separate chamber. Thus, the formation of semiconductor layers containing simultaneously three Group-V elements (As, N, Sb) is undoubtedly associated with the more complex technology of their epitaxial deposition and more complex and expensive equipment for performing the epitaxial process.

At the same time, at present there are prerequisites for raising the diffusion length of minority carriers by employing molecular-beam epitaxy to fabricate heterostructures from solid solutions of compounds containing no antimony. For example, the use of the InAs/GaAsN nanoheterostructure of original design under study makes it possible to demonstrate a high light-conversion efficiency, which compares well with the quantum efficiency of an antimony-containing InGaAsNSb cascade and surpasses that of cascades based on GaNAs and GaInAsN solid solutions.

2. EXPERIMENTAL

p–*i*–*n* Heterostructures of *p*-GaAs/*i*-(InAs/GaAsN)/*n*-GaAs test solar cells were grown by molecular-beam epitaxy in a Veeco GENIII installation, with atomic nitrogen produced by a plasma source with high-frequency (13.56 MHz) gas discharge. As substrates served *n*-GaAs (100) wafers. The layer thicknesses and doping levels are listed in the table. The total thickness of the *i*-(InAs/GaAsN) superlattice varied from 0.9 to 1.6 μm. The test solar cells under study were fabricated without an antireflection coating.

Layer parameters of the heterostructures under study

Layer	Doping level, cm^{-3}	Thickness
p^+-GaAs	10^{19}	100 nm
Wide-gap p-GaAs emitter	10^{18}	100 nm
i-(InAs/GaAsN) (E_g = 1.03 eV)	–	0.9–1.6 μm
n-GaAs	10^{18}	100 nm
n-GaAs substrate	10^{18}	

3. RESULTS AND DISCUSSION

To solve the problems associated with epitaxial growth of the InGaAsN ternary solid solution, we decided to use an InAs/GaAsN short-period superlattice as the active layer. The average lattice constant of the InAs/GaAsN superlattice nearly coincides with the lattice constant of gallium arsenide and the formation of a heterostructure of this kind on the surface of gallium arsenide does not give rise to crystal defects, such as mismatch dislocations. The distance between ultrathin layers of the narrow-gap binary compound InAs is chosen so as to provide the effective overlapping of wave functions of carriers localized at these layers within the range 6–11 nm. The thickness of ultrathin layers of the binary compound InAs was less than 0.5 nm to preclude the formation of 3D indium-arsenide layers on the epitaxial surface.

The image of the p-i–n heterostructure with a 0.9-μm-thick i-(InAs/GaAsN) region, furnished by transmission electron microscopy (TEM), in Fig. 1 shows that there are no threading dislocations and the 2D growth of InAs/GaAsN is retained. In addition, the TEM image demonstrates a smooth morphology of the layers and abrupt heterointerfaces.

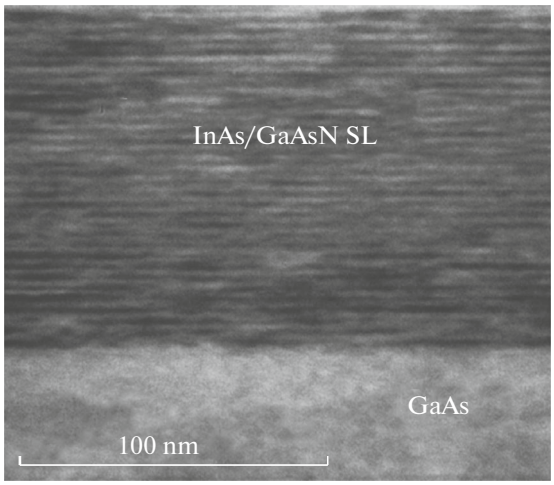

Fig. 1. TEM image of the InAs/GaAsN superlattice on an n-type GaAs layer.

The high crystal perfection of the heterostructures grown in the study is also confirmed by high-resolution X-ray diffraction analysis (HR-XRD). Figure 2 shows a rocking curve of the nanoheterostructure with an active region containing two InAs/GaAsN superlattices (SL1 and SL2) with different periods, 8 and 10 nm. The curve clearly demonstrates, in addition to the highest intensity peak corresponding to X-ray diffraction on gallium arsenide, the structure of periodic peaks –1($SL1$), –2($SL1$), +1($SL1$) and –1($SL2$), –2($SL2$), which are associated with diffraction at two different superlattices with different periods. The central peak 0($SL1$ and $SL2$) in the structure of the periodic peaks, which shows the average lattice constant in the superlattices, coincides for both superlattices and is close to the peak of gallium arsenide.

The current–voltage characteristic of the p–i–n solar-cell heterostructures without an antireflection coating is shown in Fig. 3. The upper grid of the contacts was not optimized, which led to a small fill factor FF and high dark current. The open-circuit voltage V_{oc} reached a value of 0.4 V for structures with a 0.9-μm-thick i-(InAs/GaAsN) layer, which points to the high potential of the samples obtained.

Making the i-(InAs/GaAsN) layer thicker (1.2 μm) leads to a decrease in V_{oc}, whereas a further increase in the thickness causes a substantial decrease in the short-circuit current J_{sc}. This may indicate that stress builds up between GaAs and the InAs/GaAsN superlattice for a thicker i-region layer because of imperfect matching between the average lattice constant of the superlattice and the lattice constant of GaAs.

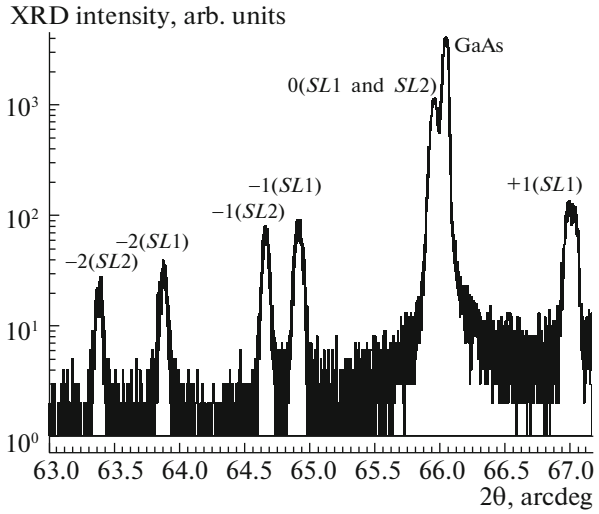

Fig. 2. X-ray-diffraction rocking curve of a nanoheterostructure with an active region containing two InAs/GaAsN superlattices $SL1$ and $SL2$ with different periods of 8 and 10 nm.

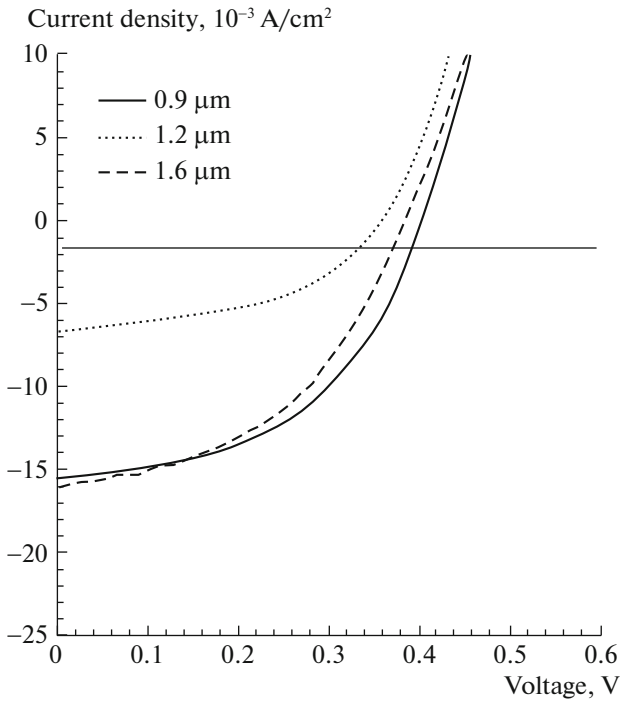

Fig. 3. Current–voltage characteristics of *p–i–n* heterostructures of *p*-GaAs/*i*-(InAs/GaAsN)/*n*-GaAs test solar cell with various *i*-region thicknesses (indicated in the figure) under AM1.5G illumination (100 mW/cm^2).

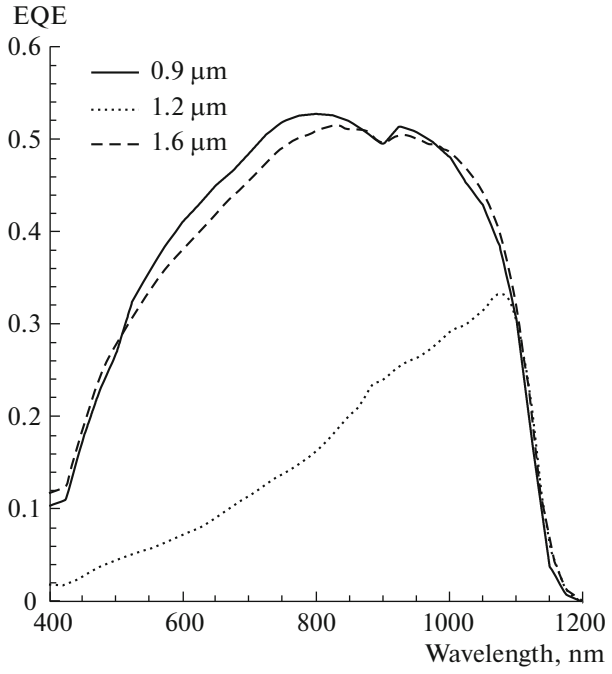

Fig. 4. EQE spectrum of *p–i–n* heterostructures of the *p*-GaAs/*i*-(InAs/GaAsN)/*n*-GaAs test solar cell with various *i*-region thicknesses (indicated in the figure).

The external quantum efficiency (EQE) spectra of *p–i–n* heterostructures with various thicknesses of the *i*-(InAs/GaAsN) region are shown in Fig. 4. It can be seen that the quantum efficiency decreases at small wavelengths with increasing thickness of the *i*-(InAs/GaAsN) layer superlattice.

Figure 5a shows the quantum efficiency (QE) spectrum at zero reflection, calculated from the EQE spectrum as EQE/(1 − *R*), where *R* is the reflectance. The quantum efficiency reaches values of 0.75 at a wavelength of 940 nm for the sample with a 0.9-μm-thick *i*-(InAs/GaAsN) region. The short-circuit current J_{sc} = 26.58 mA/cm^2 at AM1.5G. The decrease in the quantum efficiency at wavelengths exceeding 940 nm is due to the transmission loss (because of incomplete absorption).

The QE spectrum of the heterostructure under study (Fig. 5a) contains two peaks at (2) 800 and (1) 940 nm and (3) a short-wavelength shoulder at 650 nm. The reflection measurements demonstrated that the features in the QE spectra are unrelated to interference effects.

In [8], the similar shape of the quantum-efficiency spectra with two peaks for a solar cell based on another nitrogen-containing solid solution GaPNAs was attributed to the unusual structure of the conduction band of this compound, constituted by two conduction subbands E_- and E_+.

The band structure of GaInNAs, calculated in terms of the band-anticrossing model, is presented schematically in Fig. 5b [9]. The figure shows three possible transitions upon the absorption of a photon: (1) from the heavy- or light-hole *hh* (*lh*) level of the valence band to the conduction subband E_-, with an energy of 1 eV; (2) from a spin-orbit-split level of the valence band (*so*) to the E_- subband, with an energy of 1.34 eV; and (3) from the heavy- or light-hole *hh* (*lh*) level of the valence band to the E_+ subband, with an energy of 1.8 eV. The energies of these transitions are in good agreement with the energies of characteristic regions in the QE spectrum.

The long-wavelength edge of the spectral response corresponds to the transition (1) from the valence band *hh* (*lh*) to the E_- subband (1.05 eV); the long-wavelength peak (940 nm) also corresponds to this transition. With increasing energy, absorption decreases, which leads to the minimum value of the quantum efficiency at 900 nm. When the energy reaches a value sufficient for the transition (2) from the *so* level of the valence band to the E_- subband, a second QE peak appears at 800 nm. The additional absorption of light leads to the transition (3) from the *hh* (*lh*) level of the valence band to the E_+ subband and gives rise to the QE shoulder at 650 nm (3).

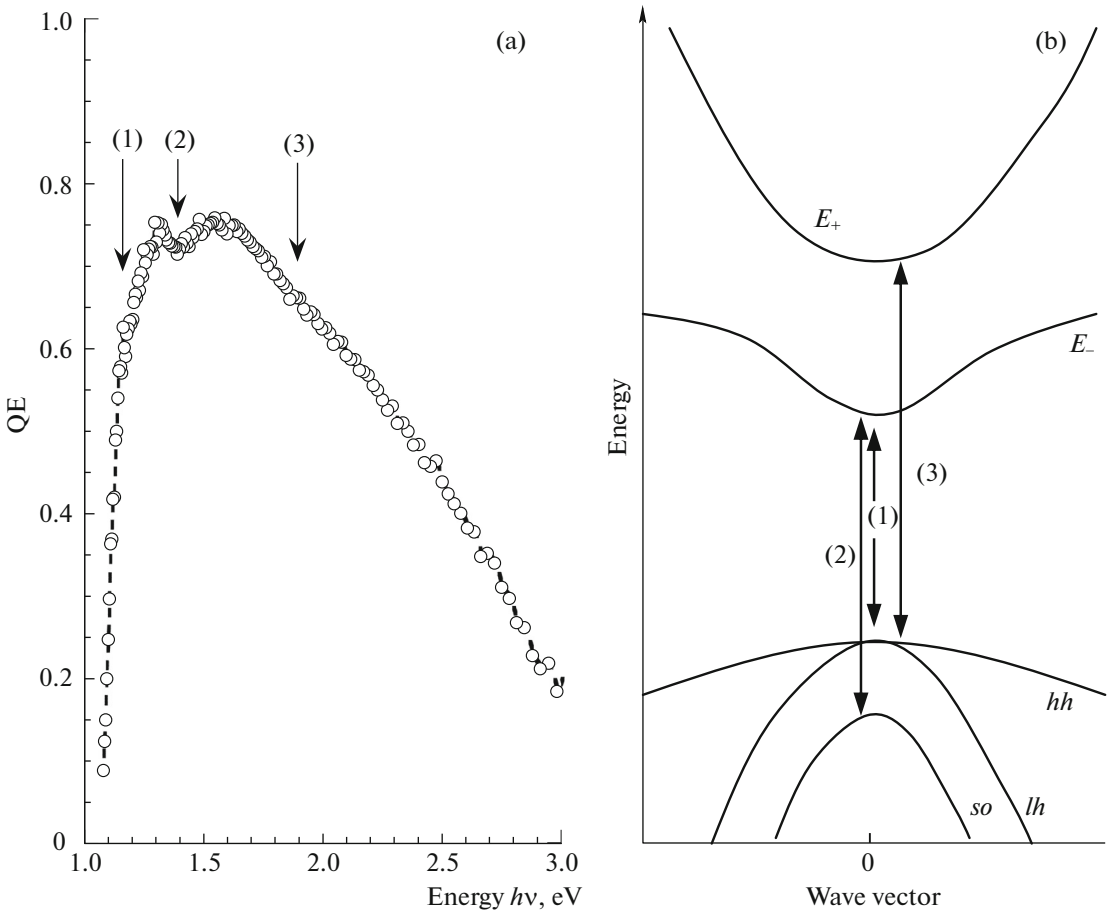

Fig. 5. (a) QE spectrum of the *p*–*i*–*n* heterostructure and (b) band diagram of the GaInNAs solid solution.

4. CONCLUSIONS

The nanoheterostructures under study have a high quantum efficiency of light conversion.

The *p*-GaAs/*i*-(InAs/GaAsN)/*n*-GaAs test solar cell with a 0.9-μm-thick *i*-(InAs/GaAsN) active layer has an open-circuit voltage of 0.4 V (under AM1.5G illumination) and a quantum efficiency exceeding 0.75 at a wavelength of 940 nm (at zero reflection loss), which corresponds to a short-circuit current of 26.58 mA/cm^2 (AM1.5G, 100 mW/cm^2).

This is due to an increase in the minority-carrier lifetime because of the decreasing density of crystal defects. This result is provided by choosing not to use solid-solution layers simultaneously containing indium and nitrogen, such as InGaAsN, but using a short-period InAs/GaAsN superlattice as the active layer. The high open-circuit voltage shows that the InAs/GaAsN superlattice as a material with a band gap of 1 eV can be used in four-cascade solar cells.

REFERENCES

1. R. R. King, D. C. Law, K. M. Edmondson, C. M. Fetzer, G. S. Kinsey, H. Yoor, R. A. Sherif, and N. H. Karam, Appl. Phys. Lett. **90**, 183516 (2007).
2. D. J. Friedman, J. F. Geisz, S. R. Kurtz, and J. M. Olson, J. Cryst. Growth **195**, 409 (1998).
3. S. R. Kurtz, A. A. Allerman, E. D. Jones, J. M. Gee, J. J. Banas, and B. E. Hammons, Appl. Phys. Lett. **74**, 729 (1999).
4. S. R. Kurtz, A. A. Allerman, C. H. Seager, R. M. Sieg, and E. D. Jones, Appl. Phys. Lett. **77**, 400 (2000).
5. A. Khan, S. R. Kurtz, S. Prasad, S. W. Johnston, and J. Gou, Appl. Phys. Lett. **90**, 243509 (2007).
6. Reported Timeline of Solar Cell Energy Conversion Efficiencies from National Renewable Energy Laboratory (National Center for Photovoltaics, USA). http://www.nrel.gov/ncpv/
7. M. A. Green, K. Emery, Y. Hishikawa, W. Warta, and E. D. Dunlop, Progr. Photovolt.: Res. Appl. **21**, 827 (2013).
8. A. I. Baranov, A. S. Gudovskih, E. V. Nikitina, and A. Yu. Egorov, Tech. Phys. Lett. **39**, 1117 (2013).
9. W. Walukiewicz, W. Shan, K. M. Yu, and J. W. Ager, in *Dilute Nitride Semiconductors*, Ed. by M. Henini (Elsevier, Amsterdam, 2005), p. 325.

Translated by M. Tagirdzhanov